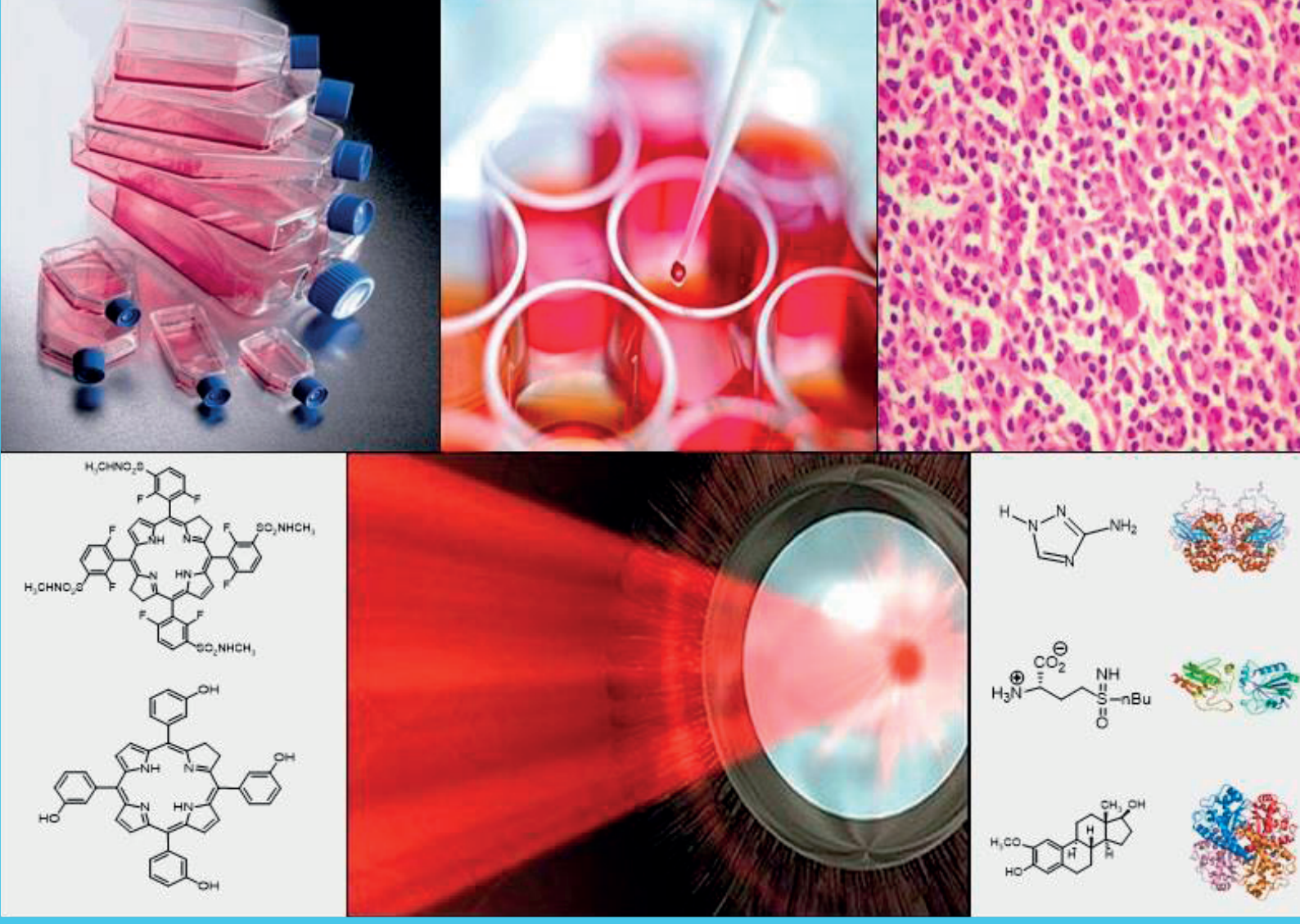

Joana Rua da Silva Campos

STRATEGIES TO ENHANCE PHOTODYNAMIC THERAPY

Master in Medicinal Chemistry

Chemistry Department
FCTUC

Junho, 2015

UNIVERSIDADE DE COIMBRA

Joana Rua da Silva Campos

STRATEGIES TO ENHANCE PHOTODYNAMIC THERAPY

Dissertation presented as evaluation for the Master in Medicinal Chemistry

Supervisor: Prof. Luis G. Arnaut

June, 2015

University of Coimbra

GRAPHICAL ABSTRACT

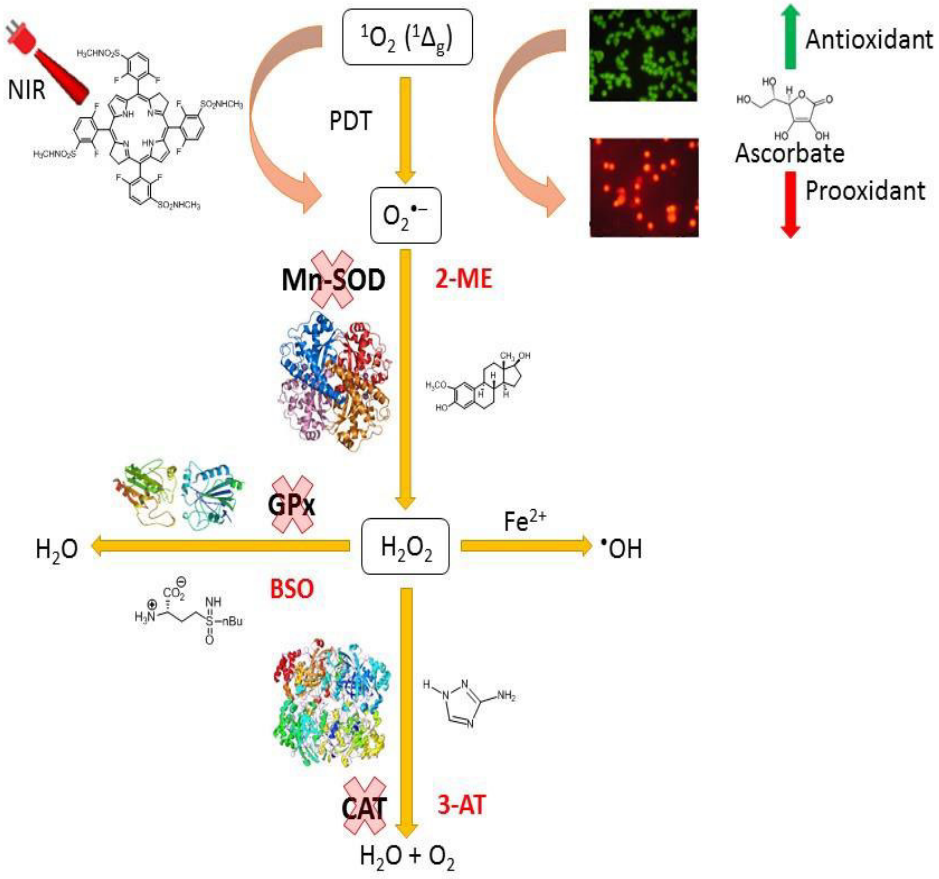

Strategies to enhance Photodynamic Therapy

Joana R.S. Campos*[1], Hélder Tão[1] and Luis G. Arnaut[1]

[1] Chemistry Department, University of Coimbra, Largo Paço do Conde, 3004-531 Coimbra, Portugal

KEYWORDS: cancer, photodynamic therapy, redaporfin, temoporfin, phototoxicity, ROS, hydroxyl radical, singlet oxygen, superoxide ion, ascorbic acid, catalase, glutathione, superoxide dismutase, glycolysis, inhibition, 3-AT, BSO, 2-ME, 2-DG, A549 cell line, CT-26WT cell line, NHI-3T3 cell line.

ABSTRACT: Photodynamic therapy (PDT) is well-known cancer treatment modality that has been used with good results and is based on the combined use of photosensitizer, light and molecular oxygen to induce cell death. The relative *in vitro* efficacy of PDT with a fluorinated bacteriochlorin, that generates singlet oxygen, hydroxyl radical and superoxide ion, or with temoporfin, which only generates singlet oxygen, depends on the superoxide dismutase (SOD) activity levels of the cell lines and depends the inhibition of glycolysis. The addition of ascorbate further potentiates phototoxicity in A549 cells, presumably by electron transfer to the radical cation of the photosensitizer and consequent increase in the turnover of radicals. The inhibition of catalase and the depletion of the glutathione pool have similar effects in A549 and CT26 cells, although less impressive in CT26. CT26 cells have a higher SOD activity level and are less sensitive to Type I processes. The phototoxicity towards CT26 cells seems to be mostly mediated through singlet oxygen and the inhibition of the cell antioxidant defence system is less effective in potentiating PDT phototoxicity. Inhibition of glycolysis leads to increased steady-state levels of ROS and enhanced cell killing by oxidative stress due to 2-Deoxy-D-glucose (2-DG) inhibit the formation of pyruvate and NADPH, which function in the detoxification pathways of H_2O_2.

ABBREVIATIONS

DMEM, Dulbeccos's Modified Eagle's medium; RPMi, Dulbeccos's Modified Eagle's medium without phenol red; PDT, photodynamic therapy; F_2BMet (or redaporfin), 5,10,15,20-tetrakis(2,6-difluoro-3-N-methylsulfamoylphenyl)bacteriochlorin; mTHPC, *m*-tetra(hydroxyphenyl)chlorin; ROS, reactive oxygen species; superoxide ($O_2^{\bullet-}$); hydrogen peroxide (H_2O_2); hydroxyl radical ($OH^{\bullet}$); CAT, catalase; 3-AT, 3-amino-1,2,4-triazole; Mn-SOD, superoxide dismutase; 2-ME, 2-metoxyestradiol; GSH, reduced form of glutathione; GSSG, oxidized form of glutathione; BSO, buthionine sulfoximine; 2-DG, 2-Deoxy-D-Glucose.

INTRODUCTION

Cancer remains one of the leading causes of death worldwide, with 10 million new cases detected every year. The management of cancer has an increasing impact in developed societies and in the world at large, as a result of technological and scientific progresses that are increasing the survival of cancer patients [1].

The normal growth and development of an organism is highly regulated, with a balance between signaling pathways that promote cell growth and pathways that promote the inhibition of growth and cell death. The disruption of this homeostasis produces pathological conditions [2]. Cancer is defined as a pathological process that occurs in several stages and involves dynamic changes of the genome. These changes provide advantages to growth and cell survival, and promote malignant transformation [3].

There has been an increase in the effectiveness of different forms of treatment and simultaneously an increase in the awareness of health professionals and the general public concerning oncologic diseases, which contribute to early diagnosis and successful treatments. The methods of treating cancer include surgery, chemotherapy, radiotherapy, immunotherapy and photodynamic therapy, among other modalities of treatment [4,5].

Conventional therapies have in common the lack of selectivity, the limited number of times they can used and the important side effects due to high toxicity to non-tumor cells. On the other hand, photodynamic therapy is minimally invasive and clinically approved for the treatment of oncological and non-oncological diseases, for example, acne, eczema, psoriasis, atherosclerosis and arthritis. It is a selective technique that depends on action of three essential components: a photosensitizer (PS), visible light and molecular oxygen. The combination of these elements, alone innocuous, triggers the production of reactive oxygen species responsible for the inactivation and destruction of tumor

cells. In most oncological applications, the photosensitizer is administered, accumulates in the tumor tissue and then the targeted tissue is irradiated with a light of a wavelength absorbed by photosensitizer. This wavelength lies typically between 650 and 850 nm (phototherapeutic window), which is the region with greater penetration into human tissue without causing damage to this because it is where tissues are the most transparent. When activated, the photosensitizer in an electronically excited state is capable of transferring an electron (Type I process) or electronic energy (Type II process) to molecular oxygen, with the concomitant formation of superoxide ion and singlet oxygen, respectively, which react with vital cellular components, leading to cell death and culminating in the destruction of the tumor [6,7]. Reactive oxygen species (ROS) such as superoxide ion and singlet oxygen, mediate the killing of tumor cells by three different mechanisms: direct cytotoxicity on tumor cells, destruction of microvasculature of the tumors through the damage caused in the endothelial cell, and stimulation of an immune response against the tumor [8].

The distribution and accumulation of the photosensitizer in the target tissue, associated with the directionality of light to this tissue, allows PDT to minimize damage to healthy tissue. PDT is a minimally invasive treatment, without side effects that may significantly affect the patients quality of life, and a single procedure may result in the necrosis of the target tissue. However, this treatment also has limitations, namely the slow clearance of some photosensitizers, the impossibility of treating non-solid tumors (e.g., leukemia), inefficient control of metastatic lesions and photosensitivity of the skin after the treatment [9,10]. Combination regimens, that include PDT and a partner treatment, should be aimed at increasing the therapeutic efficacy. In principle, this may be achieved either by counteracting the prosurvival signaling triggered in tumor cells that resisted PDT or, alternatively, by pre-weakening the tumor cells so that they become more sensitive to PDT [11]. The path followed in this thesis was to use the cellular antioxidant system and the necessity of a high level of glycolytic activity in tumor cells to enhance the efficacy of photodynamic therapy.

ROS, notably superoxide ($O_2^{\bullet-}$), hydrogen peroxide (H_2O_2) and hydroxyl radical ($OH^{\bullet}$), can damage a variety of biomolecules, for example lipids, proteins, carbohydrates and nucleic acids. Endogenous ROS production occurs primarily as a ubiquitous byproduct of both oxidative phosphorylation and a myriad of oxidases necessary to support aerobic mechanisms [12,13]. While high ROS levels are lethal to the cell, a moderate increase in ROS can promote cell proliferation and differentiation [14,15]. It has been remarked that, compared with their normal counterparts, many types of cancer cells have increased levels of ROS [16,17], and the hypothesis that tumor cells could be more vulnerable to additional production of ROS was explored by therapeutic approaches [18].

Antioxidant enzymes, such as superoxide dismutase and catalase, and the glutathione system are responsible for ROS homeostasis. Small molecules, such as ascorbate, complement the control of ROS by the antioxidant enzymes [17,19]. Several ROS generation agents are currently in clinical trials as single agents or as combination therapy [20]. An example is to treat tumor cells with pharmacological agents that have pro-oxidant properties, which increase the production of reactive species or revocation of antioxidant cellular systems. In preclinical models, agents that generate ROS showed selective toxicity in cells tumor with the increase of the ROS above the toxicity threshold that the antioxidant systems can manage [21].

Key metabolic steps for cell detoxification mechanisms are the catalysis of superoxide by superoxide dismutase (SOD) to hydrogen peroxide and oxygen, and the conversion of hydrogen peroxide to water by glutathione peroxidase (GSH-Px) or to oxygen and water by catalase (CAT). To avoid irreversible cell damage, the increased generation of ROS in cancer cells leads to positive adaptation of redox of antioxidants systems in response to oxidative stress with the purpose of restoring redox homeostasis, leading to an up-regulation of CAT, GSH and SOD [17,21]. The increase in antioxidant capacity and high levels of enzymatic activity promotes cancer cell survival and resistance to certain anticancer agents due to increased ability to remove ROS and stabilize surviving molecules through thiol modification. However, the increase of ROS makes cancer cells highly dependent on antioxidant systems, and therefore vulnerable to agents that suppress this antioxidant system. This offers a biochemical basis to selectively kill cancer cells using inhibitors of CAT, GSH and SOD. On the other hand, normal cells that have low ROS production levels and that are less dependent on antioxidant systems, can tolerate the suppression of enzymatic systems by the action of their inhibitors, such as, 3-amino-1,2,4-triazole (3-AT), buthionine sulfoximine (BSO) and 2-methoxyestradiol (2-ME), respectively [17].

Glutathione (γ-glutamyl-L-cysteinylglycine) or GSH, present in most of the cells, is the thiol (-SH) tripeptide most abundant intracellularly and is involved in cellular antioxidant defense. It consists of glutamic acid, cysteine and glycine and can be found in two forms: free or protein bound. The free form is found primarily in the reduced form (GSH), which can be converted to its oxidized form (GSSG) during oxidative stress, and can be converted back into its reduced form by the action of glutathione reductase (GR). In turn, the glutathione peroxidase (GSH-Px) catalyzes the reduction of hydrogen peroxide to water due to the conversion of GSH to GSSG [22,23]. The role of glutathione is complemented with the role of catalase, since catalase converts hydrogen peroxide to oxygen and water. Buthionine sulfoximine (BSO) is a specific inhibitor of GSH biosynthesis and does not affect other enzymes involved in the formation or removal of reactive metabolites. It is structurally identical to an intermediate of the reaction catalyzed by GCS (γ-glutamylcysteine synthetase), causing thus a decrease in the concentration of GSH [24]. This has advantages over other agents GSH inhibitors when used to demonstrate the role of GSH in toxicities induced by xenobiotics, once this inhibitor has no known toxicity to mammals and has little intrinsic chemical reactivity because only acts by inhibiting biosyn-

thesis GSH and therefore does not affect directly other cellular thiols [25]. The modulation of antioxidant redox system based on GSH, the principal determinant of the cellular redox state, may represent thus a promising therapeutic strategy for overcoming cancer progression [20].

Superoxide dismutase scavenges the reactive oxygen species (ROS), such as superoxide anion and hydroxyl radicals, and thus controls oxidative stress. Manganese superoxide dismutase (Mn-SOD) is a member of the SOD family, which includes copper and zinc-containing superoxide dismutase and extracellular superoxide dismutase. The SOD family is known to have important functions in a broad range of stress-induced pathological conditions. Among the members of the SOD family, Mn-SOD is the only enzyme that is essential for the survival of life in the aerobic environment under physiological conditions [26]. This critical function may be due to the strategic location of Mn-SOD in the mitochondria. Understanding the connection between Mn-SOD and tumorigenesis, as well as when and how Mn-SOD is modulated during cancer development, will enhance our ability to develop novel measures to intervene in the disease process [27]. 2-Methoxyestradiol (2-ME) is a physiological metabolic byproduct of the endogenous estrogen, 17β-estradiol. Recent studies demonstrated that 2-ME exerts both *in vitro* and *in vivo* anti-tumor activity against a range of solid tumors. These include breast cancer, angiosarcoma, lung cancer, pancreatic cancer, hepatocellular carcinoma, neuroblastoma and gastric cancers [19]. The modulation of antioxidant redox system based on Mn-SOD and on its inhibition with 2-ME is now considered as a promising potential anticancer agent.

Understanding the biological differences between normal and tumor cells is essential for the design and development of drugs with selective anticancer activity. Cancer cells reprogram their energy metabolism and produce energy necessary for their proliferation through glycolytic mechanism - Warburg effect [28]. Although the biochemical and molecular mechanisms that lead to increased aerobic glycolysis in tumor cells are quite complex and can be attributed to various factors, such as mitochondrial dysfunction, hypoxia and oncogenic signals, metabolic effects appear similar, so, the malignant cells need glycolysis and are dependent on this pathway to generate adenosine triphosphate (ATP). Since the generation of ATP through glycolysis is much less efficient (2 ATP per glucose) than through oxidative phosphorylation (32 ATP per glucose), the cancer cells consume much more glucose than normal cells to maintain sufficient ATP to their metabolism and active proliferation. Thus, the maintenance of a high level of glycolytic activity is essential for the survival and growth of tumor cells [21]. As this metabolic disorder is often seen in tumor cells of various tissue origins, and targeting the glycolytic pathway may preferentially kill malignant cells [27]. In normal cells, growth is regulated by external growth signals and nutrient support. Cancer cells, in contrast, have lost responsiveness to most external growth signal, and as a consequence, nutrient supply in the form of glucose likely plays a unique role in maintaining cancer cell viability. When the glycolysis is inhibited, the mitochondria, intact in normal cells, allows them to use alternative energy sources, such as fatty acids and amino acids, for the production of metabolic intermediates channeled to the TCA (tricarboxylic acid) cycle and ATP production via respiration. Recent studies have shown that inhibition of glycolysis can exert preferential effect in cells with impaired mitochondrial function due especially to cells with deletion of mitochondrial DNA and defects in breathing, leading to cell death [28].

The observation that cancer cells exhibit an increase in glycolysis and are more dependent on this pathway to generate ATP, led to the evaluation of glycolytic inhibitors as potential anticancer agents. There are several compounds that inhibit or suppress the glycolytic pathway [28,29]. 2-Deoxy-D-glucose (2-DG) is a glucose analog and has long been known to act as a competitive inhibitor of glucose metabolism. Upon transport into the cells, 2-DG is phosphorylated by hexokinase to 2-deoxyglucose-P (2-DG-P). 2-DG-P is trapped and accumulated in the cells, leading to inhibition of glycolysis mainly at the step of phosphorylation of glucose by hexokinase. Inhibition of this rate-limiting step by 2-DG causes a depletion of cellular ATP, leading to blockage of cell cycle progression and cell death *in vitro* [30]. *In vitro* studies show that 2-DG exhibits cytotoxic effect in cancer cells, especially those with mitochondrial respiratory defects or cells in hypoxic environment [31]. 2-DG produced a four to five fold greater effect in anaerobically growing cells than in aerobically growing cells. The consequences of glycolysis blocking are different in aerobic and hypoxic cells. In the aerobic cell, upon inhibition of glycolysis is by 2-DG, ATP cannot be generated by this pathway. However, since O_2 is available to the mitochondria, amino and/or fatty acids can act as energy-providing carbon sources for oxidative phosphorylation (OxPhos) to take place, producing ATP. In contrast, when glycolysis is blocked in the hypoxic cells, the other carbon sources cannot be used by mitochondria because O_2 is unavailable, and OxPhos cannot take place. Thus, when glycolysis is blocked in the hypoxic cell, it has no alternative means for generating ATP and, therefore, will eventually succumb to this treatment [29]. Competition between 2-DG and glucose is thought to cause inhibition of glucose metabolism, thereby creating a chemically induced state of glucose deprivation. It is proposed that the extent to which tumor cells increase their metabolism of glucose is predictive of tumor susceptibility to glucose deprivation induced cytotoxicity and oxidative stress. Therefore, when deprived of glucose using 2-DG, tumor cells with high glucose utilization will be more sensitive to cell death resulting from respiratory dependent metabolic oxidative stress than tumor cells with low glucose utilization and normal cells. It was hypothesized that the reason for this is because cancer cells with high glucose utilization generate more O_2 and H_2O_2 from their mitochondrial electron transport chains [32]. 2-DG competitively inhibits metabolism of glucose and has been suggested to be selectively cytotoxic to fully transformed cells, via a mechanism that involves hydroperoxide-mediated oxidative stress. Since glucose is a major source of

electrons for hydroperoxide metabolism and tumor cells are believed to produce relatively high steady-state levels of hydroperoxides, the mechanism by which 2-DG enhances oxidative stress in cancer cells was suggested to involve limitation of hydroperoxide detoxification [33]. Glucose deprivation would be expected to cause metabolism to shift to oxidative phosphorylation in order meet the metabolic demand for ATP. This shift to mitochondrial respiration would be expected to increase one electron reduction of oxygen from electron transport chains, leading to increased superoxide ($O_2^{\bullet-}$) and hydrogen peroxide (H_2O_2) fluxes. Increases in $O_2^{\bullet-}$ and H_2O_2 would then be occurring in a low glucose environment where less nicotinamide adenine dinucleotide phosphate (NADPH) was being produced through the pentose phosphate cycle and less pyruvate would be produced from glycolysis. Both NADPH and pyruvate are integrally related to hydroperoxide metabolism and detoxification. Therefore, we hypothesize that mitochondrial electron transport chain production of $O_2^{\bullet-}$ and H_2O_2 as well as organic hydroperoxides derived from the oxidation of lipids would contribute to the oxidative stress seen during glucose deprivation [34]. Since 2-DG would be expected to inhibit the formation of pyruvate and NADPH, which function in the detoxification pathways of H_2O_2, we hypothesized that the inhibition of glycolysis would lead to increased steady-state levels of ROS and enhanced cell killing by oxidative stress. The biochemical rationale for this combination to enhance cancer cell killing was based on previous results in other human cancer cells suggesting that 2-DG would inhibit glucose metabolism leading to a reduction in intracellular pyruvate and NADPH, limiting the capacity of the tumor cells to metabolize hydroperoxides and enhancing oxidative stress.

The aim of this study is use photodynamic therapy with 5 μM of a recently described fluorinated sulfonamide bacteriochlorin photosensitizer (redaporfin) to increase in ROS in cells, and explore its combination with the inhibition of glutathione peroxidase (600 μM BSO), superoxide dismutase (3 μM 2-ME) or glycolysis (2 mM 2-DG), in A549 (human lung adenocarcinoma), CT26 (mouse colon adenocarcinoma) and NIH-3T3 fibroblast cell lines, by evaluation of the impact of the combination on the cellular survival.

EXPERIMENTAL SECTION

Reagents

The culture medium (DMEM, Dubbelco's Modified Eagle's Medium) was obtained from Sigma Life Sciences. The fetal bovine serum and antibiotics (penicillin and streptomycin) were obtained from Invitrogen. The photosensitizers used, redaporfin is a halogenated bacteriochlorin (5,10,15,20-Tetrakis (2,6-fluoro-3-N-methylsulphamoylphenyl) bacteriochlorin) and it was kindly provided by Luzitin SA (Coimbra, Portugal) in sealed vials. Stock solutions of redaporfin were prepared in ethanol (≈ 1 mM) shortly before the addition to the cell cultures. BSO and 2-ME (SigmaAldrich) solutions were prepared in saline phosphate buffer (PBS) and 2-DG (SigmaAldrich) was prepared in DMEM. All incubations and washes prior to PDT were carried out under subdued light. Temoporfin (5,10,15,20-tetrakis(3-hydroxyphenyl) chlorin) was purchased from Chembest (China). Stock solutions of temoporfin were also prepared in ethanol (≈ 1 mM) shortly before the addition to the cell cultures.

Cell lines

The cell lines used were A549, human lung adenocarcinoma cancer cell line, CT26, mouse colon adenocarcinoma cancer cell line and NHI-3T3, fibroblasts cell lines. The culture medium for the cell growth used Dulbecco's Modified Eagle's Medium – high glucose (DMEM), 4-(2-hydroxyethyl)piperazine-1-ethanesulfonic acid buffer (HEPES) and sodium bicarbonate purchased from SigmaAldrich. DMEM was supplemented with 100 units/ml of penicillin (PS) (1%), 100 μg/ml streptomycin and 10% heat-inactivated fetal bovine serum (FBS) were purchased from Gibco. Unless otherwise mentioned, all cell lines were maintained at 37°C in a humidified atmosphere containing 5% CO_2 while cultured. MilliQ water was deionized with a Millipore Milli-Q water purification system.

Dark toxicity

For each experiment, cells were grown in triplicate at a density of 10.000 cells/well (A549) and 7.000 cells (CT26 and NHI-3T3) per well in 200 μl growth medium in 96-well tissue culture plates, and allowed to reach at least 80% of confluence. The cytotoxicity in the dark was independently measured after incubation of A549 and CT26 cells with BSO (100-600 μM), 2-ME (1-5 μM) and 2-DG (500 μM-100 mM) for 24 hours at 37 °C. Approximately 18 hours after incubation with drug photosensitizer, cells were washed with PBS and then incubated with a 10% solution of Resazurin and analyzed using a multi-mode micro plate reader Synergy HT™ from BioTek®. Resazurin fluorescence was measured in the following day at the emission wavelength of 590 nm. Cells were always assayed for viability 24 h after the end of the incubation periods.

In vitro generation of cell death

PDT employed as light source a LED from Marubeni (model L740-66-60-550), with an output power of 410 μW, emission maximum at 740 nm with FWHM = 25 nm. For each experiment, cells were grown in triplicate at a density of 10.000 cells/well (A549) and 7.000 cells (CT26 and NHI-3T3) per well in 200 μl growth medium in 96-well tissue culture plates, and allowed to reach at least 80% of confluence. In a standard PDT experiment, the cell lines were first incubated for 20 h with 5 μM redaporfin from an ethanol stock solution, incubated for 1 h with the BSO and 2-ME or 1, 3, 6, 12 h with 2-DG; or cell lines were first incubated with 500 μM-2 μM 2-DG and after 24 h cell lines were incubated with 5 μM redaporfin. Before exposure to the light source, the cells were rinsed with PBS and fresh medi-

um was added. A549 cell were exposed to a light dose of 40 mJ/cm^2, CT26 to a light dose of 100 mJ/cm^2 and NHI-3T3 to a light dose 50 mJ/cm^2. These light doses were selected on the basis of exploratory studies to find the light doses that killed 40-60% of the cells incubated with 5 µM redaporfin. Cells were always assayed for viability 24 h after PDT.
Statistical analyses were performed with Student's t-test for unpaired data with unequal variance, and used no less than three independent measurements.

Comparison between redaporfin and temoporfin

The comparison between redaporfin and temoporfin was made under irradiation with a homemade device using LEDs from Avago Technologies model HLMP-CE13-35CDD LED with an output power of 50 µW and emission maximum at 505 nm and FWHM = 30 nm. The light doses were calibrated to produce 40-60% of cell death in both cell lines after incubation for 20 h with 5 µM redaporfin or 500 nM temoporfin.
The light devices output powers were measured with power meter LaserCheck from Coherent.

RESULTS

Different cell lines exhibit different enzymatic activities of antioxidant systems. The path followed in this thesis was, based on previous results from our group, to inhibit the cellular antioxidant system, notably glutathione pool and superoxide dismutase, and enhance the efficacy of photodynamic therapy.
Previous results of the group showed that ascorbic acid plays a special role in cancer treatment, once it behaves in two different ways. It acts as a pro-oxidant in combination with redaporfin-PDT of A549 cells increasing the effectiveness of PDT but acts as an antioxidant in redaporfin-PDT of CT26 cells protecting them from ROS. The resistance of A549 cells to ascorbate suggests a better management of hydrogen peroxide. The oxidative stress of H_2O_2, produced either through Type I processes and/or by ascorbate, and its detoxification by catalase were evaluated in the presence of its inhibitor 3-AT in a range of 50–500 µM. The inhibition of catalase potentiates the phototoxicity of redaporfin towards A549 cells but not towards CT26 cells. The effect of adding ascorbate to redaporfin-PDT incubated with 3-AT is the same for A549 cells as that described for the addition of ascorbate to redaporfin-PDT with or without ascorbate: the survival of A549 decreases. On the other hand, it is necessary to increase the concentration of 3-AT to counter the protective effect of ascorbate in CT26 cells. The role of ascorbate as a pro-oxidant in A549 cells and an antioxidant in CT26 cells is apparent even when catalase is inhibited. The differential effect of ascorbate and 3-AT in A549 and CT26 cells motivated the assessment of the catalase activity in these cell lines. The higher toxicity of ascorbate towards CT26 cells is consistent with the lower catalase activity level in these cells. Interestingly, the more 3-AT-sensitive A549 cells have a higher catalase activity than the CT26 cells [29,35] , showing that the behavior of these cell lines to the imposed oxidative stress could not be totally explained by the catalase activity.

Depletion of intracellular glutathione with buthionine sulfoximine (BSO)

The role of the glutathione pool in the detoxification of ROS was investigated using BSO, a specific inhibitor of glutathione synthesis that is not cytotoxic (see Figure 5 Supplementary Information) in the 100-600 µM concentration range employed in this study. Figure 1 shows that the inhibition of γ-glutamylcysteine synthetase has a similar impact on the phototoxicity of redaporfin as the inhibition of catalase.

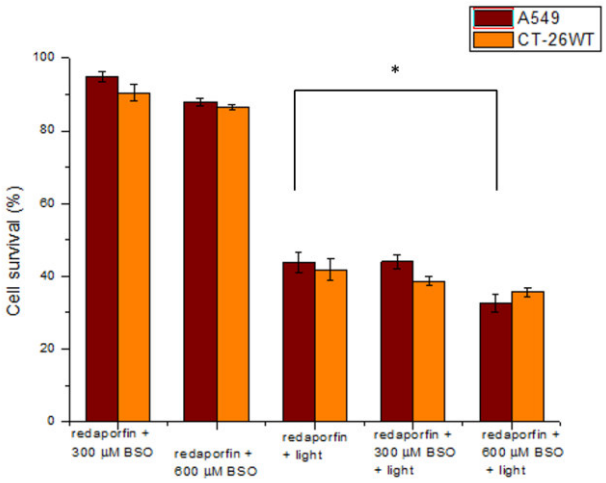

Figure 1. Dark toxicity BSO and phototoxicity of redaporfin (5 µM) alone and in combination with BSO (300 µM or 600 µM). Statistically significant difference * refer to $p<0.05$.

Figure 2 shows comparable levels of oxidized (GSSG) and reduced (GSH) forms of glutathione in A549 and CT26 cells. The ratio between the reduced and oxidized forms of glutathione is usually presented to indicate the susceptibility of the cell line or tissue to resist to oxidative stress [36]. The GSSG/GSH ratios were $(7.1\pm0.8)x10^2$ for A549 and $(7.5\pm0.6)x10^2$ for CT26 cell lines, which indicate similar glutathione activity [29].

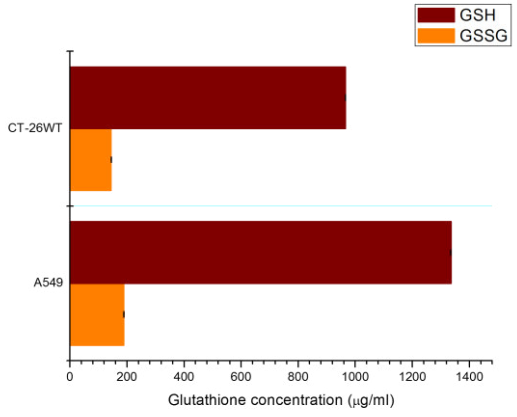

Figure 2. Pool of oxidized (GSSG) and reduced (GSH) forms of glutathione.

Inhibition of Mn-SOD with 2-metoxyestradiol (2-ME)

The role of superoxide ions in phototoxicity was investigated with the inhibition of Mn-SOD with 3 µM 2-ME. Figure 3 shows that 2-ME potentiates the effect of redaporfin-PDT in A549 cells but not in CT26 cells.

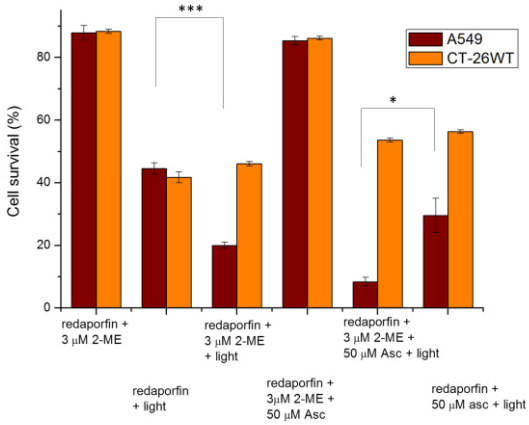

Figure 3. Dark toxicity of 2-ME and phototoxicity of redaporfin (5 µM) alone and in combination with 2-ME (3 µM). Statistically significant difference * refer to $p<0.05$ and *** to $p<0.001$.

The remarkable ability of 2-ME to potentiate PDT with A549 cells but not with CT26 cells should be interpreted in terms of the SOD activity levels of these cell lines (see Figure 4). The lower SOD activity of A549 cells leaves these cells vulnerable to superoxide ion when Mn-SOD is inhibited by 2-ME and even more in presence of both SOD inhibitor and ascorbate.

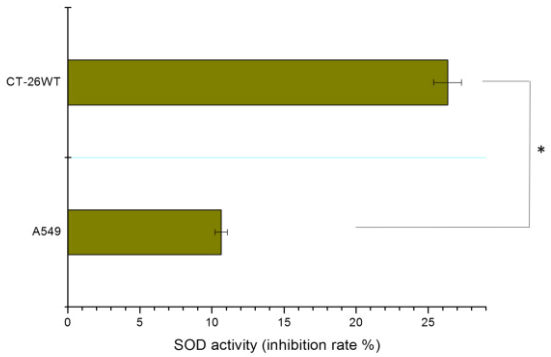

Figure 4. SOD activity. Statistically significant difference * refer to $p<0.05$.

Phototoxicities of redaporfin and temoporfin alone

For a comparison between two photosensitizers used in PDT, the redaporfin and temoporfin, in order to study the resistance of the A549 and CT26 cell lines to the superoxide ion.

Incubation with 5 µM redaporfin does not lead to measurable cytotoxicity. Figure 5 shows that the relative photoxicities of redaporfin and temoporfin towards A549 and CT26 cells are different. Whereas 0.5 µM of temoporfin need 20 mJ/cm^2 at 505 nm to kill 50% of A549 cells, only 5 mJ/cm^2 kill the same percentage CT26 cells, and precisely the opposite of the trend observed with 5 µM of redaporfin: 250 mJ/cm^2 kill 50% of A549 cells, but 500 mJ/cm^2 are needed to kill 50% of CT26 cells. This is consistent with the difference in phototoxicities previously found for HT-29 and CT26 cells [20]. Considering that the photoxicity of temoporfin is assigned to singlet oxygen [37], these results suggest that A549 cells are more sensitive to free radicals generated in Type I processes.

a)

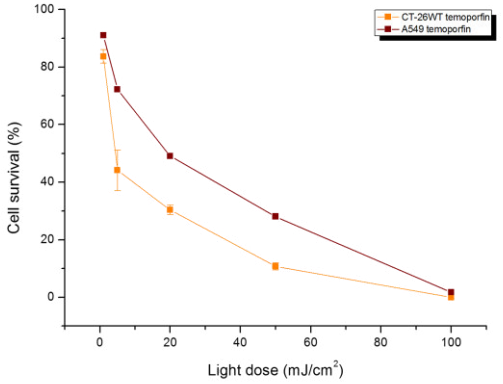

b)

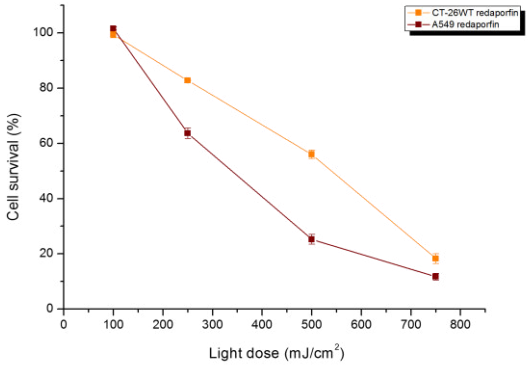

Figure 5. Photoxicity of 0.5 µM temoporfin (a) and 5 µM redaporfin (b) towards A549 (brown) and CT-26WT (orange) cells as a function of the light dose at 505 nm.

Inhibition of glycolysis with 2-Deoxy-D-glucose (2-DG)

The strategy of targeting the energy of the tumor metabolism was studied focusing on the role of the glycolysis activity in both cancer and normal cell lines. 2-DG, a specific inhibitor of glycolysis was employed in combination with

PDT, investigating a possible synergistic effect of the combination, and an increased selectivity in the therapy between normal and cancer cells. This required assessing the range of 2-DG concentrations that do not present cytotoxicity for the desired incubation times.

Figure 6 shows a protective effect in these cell lines when the cells were first incubated with 5 µM redaporfin and after 24 h incubation time were incubated with 5 mM 2-DG in the A549 and NHI-3T3 cell lines and 10 mM 2-DG in the CT26 cell line for 1, 3, 6 and 12 h before PDT.

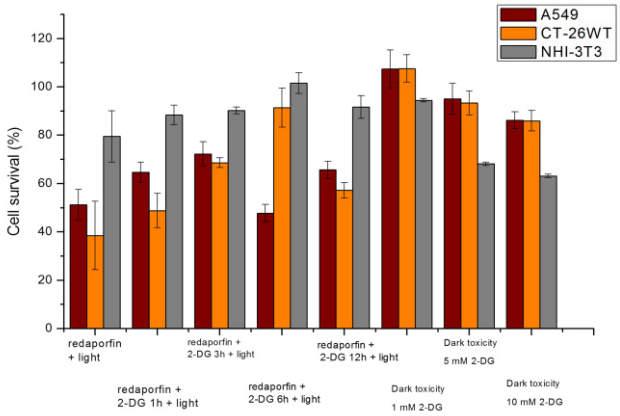

Figure 6. Dark toxicity of 2-DG during 24 h and phototoxicity of redaporfin (5 µM) alone and in combination with 2-DG (5 and 10 mM) during 1, 3, 6 and 12 h before PDT.

The toxicity of 5 µM redaporfin with 5 and 10 mM 2-DG for 48 h was assessed and proved to be significant toxic (see Figure 6 supplementary information). The toxicity of 5 µM redaporfin with 500 µM-2 mM 2-DG during 48 h was tested and proved to be not cytotoxic (see Figure 7) in concentration range employed in this study.

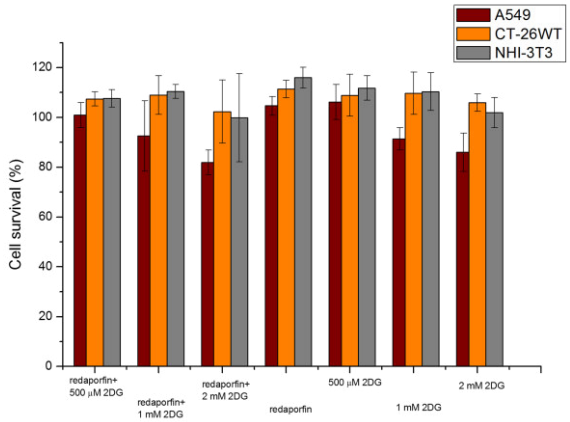

Figure 7. Dark toxicity of 5 µM redaporfin with 500 µM–2 mM 2-DG during 48 h.

The phototoxicity of 5 µM redaporfin with 500 µM-2 mM 2-DG during 48 h was tested and was found significant toxicity in this concentration range.

Therefore, the study was focused on the inhibition of glycolysis for 48 h with 2-DG in this concentration range.

Figure 8 shows an increased effect in PDT-induced cytotoxicity concentration dependent of inhibitor in cancer cells when glycolysis was inhibited for 48 h before PDT. The premise that tumor cells are more susceptible to glycolysis inhibition than fibroblasts remains questionable. For inhibitor concentrations of 1 mM but the selectivity was not found but for higher amounts of inhibitor it seems that is possible to promote a differential treatment.

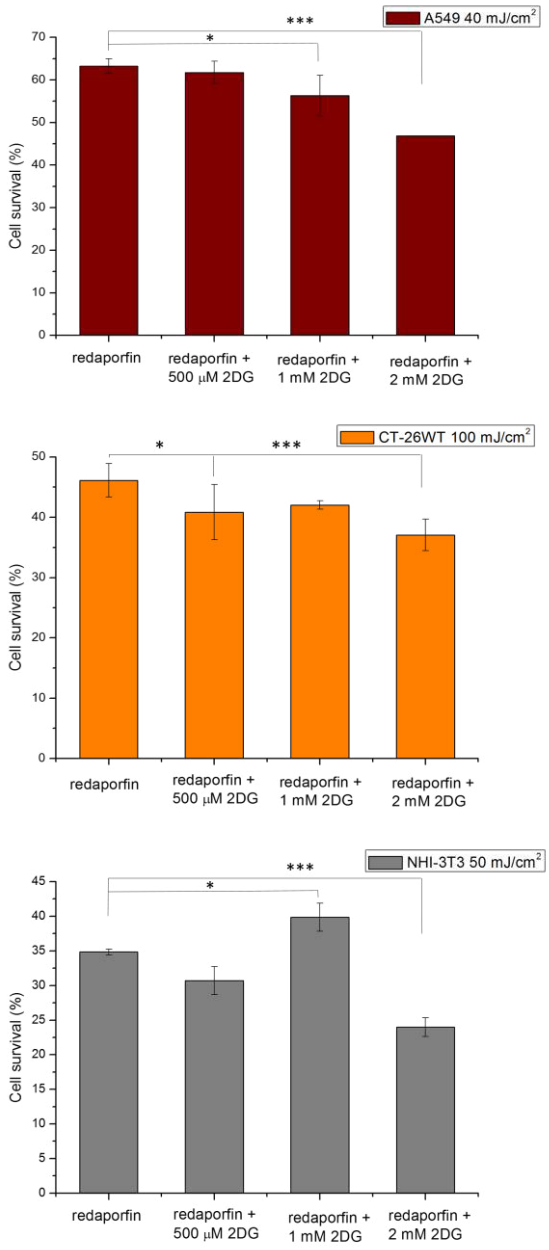

Figure 8. Phototoxicity of 5 µM redaporfin (incubated 20 h) alone and in combination with 500 µM–2 mM 2-DG (incubated 48 h before PDT). Statistically significant difference * refer to $p<0.05$ and *** to $p<0.001$.

DISCUSSION

Redaporfin is characterized by a strong light absorption at 749 nm in CrEL:ethanol:NaCl 0.9 % (0.2:1:98.8, v:v:v) solution, $\varepsilon_{748}=1.25\times10^5$ M^{-1} cm^{-1} [16] and has the ability to

transfer an electron to molecular oxygen and generate superoxide ions and hydroxyl radicals in aqueous solutions. It is a promising photosensitizer for PDT and a useful tool to explore the roles of Type I and Type II processes in phototoxicity. The fluorescence intensities of redaporfin in A549 and CT26 cells after 24 h of incubation were not significantly different. The phototoxicity differences between these cell lines are probably not related to the uptake of redaporfin.

A very important observation is that ascorbate acts as a pro-oxidant in combination with redaporfin-PDT of A549 cells but acts as an antioxidant in redaporfin-PDT of CT26 cells. Ascorbate changes from a pro-oxidant in the dark to an antioxidant when redaporfin is irradiated in CT26 cells [35]. Redaporfin, (F_2BMet in equations), is nearly insoluble in water and localizes preferentially in the endoplasmic reticulum (ER). Molecular oxygen is also much more soluble in organic solvents than in water. Thus, triplet redaporfin undergoes diffusion-controlled energy and electron transfer reactions with molecular oxygen mostly in the ER

$$^3F_2BMet + O_2 \rightarrow F_2BMet + {}^1O_2 \quad (1)$$
$$^3F_2BMet + O_2 \rightarrow F_2BMet^{\bullet+} + O_2^{\bullet-} \quad (2)$$

Type I reactions with biomolecules are also possible but will not be considered here for simplicity. The radical cation $F_2BMet^{\bullet+}$ should then move to a more polar environment where it can be reduced by water-soluble ascorbate

$$F_2BMet^{\bullet+} + AH^- \rightarrow F_2BMet + AH \quad (3)$$

The rapid regeneration of F_2BMet can prevent the decomposition of its radical cation. The increase in photostability with reaction 3 allows for additional cycles of reactions 1 and 2. This mechanism explains the pro-oxidant effect of ascorbate in combination with F_2BMet-PDT observed with A549 cells. The superoxide ion is in equilibrium with the perhydroxyl radical ($HO_2 \rightleftarrows O_2 + H^+$, p$K$=4.8) in aqueous solution and both react with ascorbic acid/ascorbate

$$HOO^{\bullet}/O_2^{\bullet-} + AH_2/AH^- \rightarrow H_2O_2 + A^{\bullet-} \quad (4)$$

with a rate constant k_4=3x10^5 M^{-1} s^{-1} [38]. The dismutation of the superoxide ion by superoxide dismutase

$$Mn^{3+}\text{-SOD} + O_2^{\bullet-} \rightarrow Mn^{2+}\text{-SOD} + O_2 \quad (5a)$$

$$Mn^{2+}\text{-SOD} + O_2^{\bullet-} + 2H^+ \rightarrow Mn^{3+}\text{-SOD} + H_2O_2 \quad (5b)$$

is much faster, ≈10^9 M^{-1} s^{-1} [38], but for high local concentrations of ascorbate reaction 4 could explain part of the antioxidant effect of ascorbate in combination with F_2BMet-PDT observed with CT26 cells.

We propose that singlet oxygen is the pivotal ROS in phototoxicity towards CT26 cells for the following reasons (i) the phototoxicity of temoporfin is mediated by singlet oxygen and the phototoxicity of temoporfin is higher towards CT26 cells than A549 cells, (ii) redaporfin generates both superoxide ions and singlet oxygen and is less phototoxic towards CT26 cells than A549 cells, (iii) the inhibition of γ-glutamylcysteine synthetase depletes the glutathione pool that protects cells against free radicals but has little effect on the phototoxicity of redaporfin towards CT26 cells, and (iv) the inhibition of Mn-SOD increases intracellular superoxide ions but has little effect in the phototoxicity of redaporfin towards CT26 cells. The resistance of CT26 cells to Type I processes is certainly related with their high level of SOD activity. CT26 cells can efficiently manage the oxidative stress caused by superoxide ions by converting them to H_2O_2 with SOD. Next, these cells upregulate catalase to detoxify H_2O_2 and maintain their resistance against Type I reactions.

A549 cells have a higher sensitivity to Type I processes. This is assigned to a low SOD activity level that makes these cells especially sensitive to elevated levels of superoxide ion. The inhibition of Mn-SOD increases the oxidative stress by radical species and is accompanied by a strong increase in the phototoxicity of redaporfin towards A549 cells. The depletion of the glutathione pool also leads to some potentiation of redaporfin-PDT towards A549 cells. The most striking result of the combinations of redaporfin-PDT with the various inhibitors is that a very strong potentiation of PDT is possible when Type I processes determine phototoxicity. It is more difficult to potentiate PDT when Type II processes control phototoxicity.

The ability of singlet oxygen to explore the whole cell reflects a cytotoxicity that is weakly dependent on the regulation of oxidative stress by the cells. On the other hand, the cascade of radical reactions initiated by electron transfer from the photosensitizer to molecular oxygen leads to superoxide ions and hydrogen peroxide that are managed by specific cellular defense mechanisms. When these ROS escape such defenses, they can lead to hydroxyl radicals that have a 1 ns lifetime in cells and can produce damage over a range of 1 nm [39]. Very reactive radicals produce cellular damage within the organelles where they are formed and only a large glutathione pool can offer some protection.

In general, cancer cells exhibit increased glycolysis and pentose-phosphate cycle activity, while demonstrating only slightly reduced rates of respiration. These metabolic differences were initially thought to arise as a result of "damage" to the respiratory mechanism, and tumor cells were thought to compensate for this defect by increasing glycolysis. However, if cancer cells increase glucose metabolism to form pyruvate and nicotinamide adenine dinucleotide phosphate (NADPH) as a compensatory mechanism, in response to ROS formed as byproducts of oxidative energy metabolism, then inhibition of glucose metabolism would be expected to sensitize cancer cells to agents that increase levels of hydroperoxides (i.e., ionizing radiation and chemotherapy agents). Studies have shown that glucose deprivation can induce cytotoxicity in transformed human cell types via metabolic oxidative stress. Glucose analogues, such as 2-DG, have been found to profoundly inhibit glucose metabolism in cancer cells *in vitro* and *in vivo* [33].

2-DG has been proven to be an effective inhibitor of cell metabolism and ATP production. 2-DG is a structural analogue of glucose differing at the second carbon atom by the

substitution of hydrogen for a hydroxyl group (see Figure 2 Supplementary Information) and appears to selectively accumulate in cancer cells by metabolic trapping because of increased uptake, high intracellular levels of hexokinase or phosphorylating activity, and low intracellular levels of phosphatase (see Figure 3 Supplementary Information) [32,33]. Two properties of 2-DG, namely, the inhibition of glycolysis and the preferential accumulation in cancer cells, have formed the basis for further investigating the mechanism of 2-DG for its use as an antitumor agent. It has been speculated that cancer cells initially treated with 2-DG exhibit a stress response caused by a depletion of intracellular energy. The stress response results in increased levels of glucose transporter expression and increased glucose uptake, which allow more 2-DG to enter the cell. As a consequence of high intracellular 2-DG concentrations, hexokinase and hexose phosphate isomerase are inhibited, energy stores such as ATP are further depleted and, finally, the cell activates the cell death pathway [40]. In addition, increased prooxidant production and profound disruptions in thiol metabolism consistent with metabolic oxidative stress were also noted in cancer cells during glucose deprivation or when treated with the glucose analogue 2-DG [41]. Studies have shown that the cytotoxic effect of 2-DG is heterogeneous among different tumor cell lines. While profound growth inhibition and cell death have been found in some cells, a marginal effect on growth and clonogenicity have also been reported in a few. A number of factors contribute to these two diversified responses, which includes the extent of glucose dependence and glycolysis, energy deprivation in the form of ATP depletion and imbalance in the oxidative stress (mitochondrial metabolism). Cell death, induced by 2-DG, could be either apoptotic or necrotic depending on the cell type and environmental factors. The relationship between enhanced glycolysis and apoptotic cell death due to glucose deprivation induced by 2-DG remains to be elucidated, although alteration in the redox state due to a decrease in the regeneration of NADH and lactate by inhibition of glycolysis has been proposed to trigger the final apoptotic pathway [42].

We saw that 2-DG was initially protective against PDT when applied for 1 – 12 h, presumably because 2-DG can acts as anti-oxidant or a *quencher* of redaporfin. For long 2-DG incubation time (> 48h), there is evidence that cancer cells become more sensitive to PDT, however 2-DG do not show significant selectivity between tumor cells and fibroblasts in the conditions explored in this work.

CONCLUSION

The phototoxicity of photosensitizers capable of transferring an electron to molecular oxygen is higher towards cell lines with low SOD activity levels. Moreover, in this combination of photosensitizer-cell line it is possible to potentiate phototoxicity with the inhibition of Mn-SOD. This potentiation may improve the outcome of PDT with redaporfin and spare healthy tissues.

Singlet oxygen causes oxidative stress in the whole cell and reacts selectively, while the hydroxyl radicals resulting from the chain of Type I processes have spatial specificity. Photosensitizers that combine Type I and Type II processes offer better opportunities to potentiate their PDT efficacy, especially through the inhibition of the enzymes of the cell antioxidant defense system.

Understanding the biological differences between normal and cancer cells is essential for the design and development of drugs with selective anticancer activity. The maintenance of a high level of glycolytic activity is essential for tumor cells to survive and grow. As this metabolic disorder is often seen in tumor cells of various tissue origins, targeting the glycolytic pathway may preferentially kill malignant cells and, probably, have general therapeutic implications. We have shown that the inhibition of glycolysis can enhance PDT but selectivity between tumor cells and fibroblasts has yet to be found. In the future we want to study the inhibition of glycolysis in epithelial cells, perform *in vivo* studies and, possibly, consider other inhibitors of glycolysis [29] to maximize the impact of the therapy in cancer cells without damage healthy cells.

AUTHOR INFORMATION

Corresponding Author

* Joana Rua da Silva Campos
joanacampos92@gmail.com
Department of Chemistry at University of Coimbra
Largo Paço do Conde, 3004-531 Coimbra, Portugal

ACKNOWLEDGMENT

It is acknowledged financial support from the Department of Chemistry at University of Coimbra, financially supported by the Portuguese Science Foundation (FCT) with project PEst-OE/QUI/UI0313/2014 and also supported with project PTDC/QUI-QUI/120182/2010. It is also acknowledge all the support from the Structure, Energy and Reactivity group at University of Coimbra, especially Hélder Tão Ferraz Cardoso Soares, MSc and Professor Luis Guilherme da Silva Moreira Arnaut, PhD I want to thank you for all the support, guidance and teachings provided along the realization of this project.

REFERENCES

[1] Garcia, M.; et al. Atlanta, GA: American Cancer Society; 2007.
[2] Bertram, J. *Mol Aspects Med* **21:** 167–223; 2001.
[3] Weinberg, R. *Garland Science*; 2007.
[4] Goodson, AG.; Grossman, D. *J Am Acad Dermatol* **60**: 719-735; 2009.
[5] Hodi, FS; O'Day, SJ; McDermott, DF. *N Eng J Med* **363**: 711-723; 2010.
[6] Pineiro, M.; Pereira, M.; Arnaut, L. *J. Photochemistry and Photobiology* **138**: 147–157; 2001.
[7] Nyman E.; Hynninen P. *J. Photochem Photobiol B* **73**: 1-28; 2004.
[8] Denis, TGS; Aziz, K; Waheed, AA; Huang, YY; Sharma, SK; Mroz, P; Hamblin, MR; *Photochemical Photobiological Sci* **10**: 792-801; 2011.

[9] Josefsen B.; Boyle, W. Brit. *B. J. Pharmacol* **154**: 1-3; 2008.
[10] Triesscheijn, M.; et al. *The Oncologist* **11(9):** 1034-1044; 2006.
[11] Verma, S.; Watt, G. M.; Mai, Z.; Hasan, T. *Photochem. Photobiol.* **83:** 996-1005; 2007.
[12] Cohen, MV. *Ann Intern Med* **111**: 918-31; 1989.
[13] Boonstra, J.; Post, J. A. *Gene* **337**: 1-13; 2004.
[14] Silva, E. F. F.; Serpa, C.; Dabrowski, J. M.; Monteiro, C. J. P.; Arnaut, L. G.; Formosinho, S. J.; Stochel, G.; Urbanska, K.; Simoes, S.; Pereira, M. M. *Chem. Eur. J.* **16**: 9273-9286; 2010.
[15] Schafer, F. Q.; Buettner, G. R. *Free Radical Biol. Med.* **30**: 1191-1212; 2001.
[16] Szatrowski, T. P.; Nathan, C. F. *Cancer Res.* **51**: 794-798; 1991.
[17] Trachootham, D.; Alexandre, J.; Huang, P. *Nature Rev. Drug Discovery* **8(7)**: 579-591; 2009.
[18] Wang, J.; Yi, J. *Cancer Biol. Ther.* **7:** 1875-1885; 2008.
[19] Kramarenko, G.; Wilke, W.; Dayal, D.; Buettner, G..; Schafer, F. *Free Radic Biol Med* **40(9):** 1615–1627; 2006.
[20] Arnaut, L.G.; Pereira, M.M.; Dabrowski, J.M.; Silva, E.F.F.; Schaberle, F.A.; Abreu, A.R.; Rocha, L.B.; Barsan, M.M.; Urbanska, K.; Stochel, G.; Brett, C.M.A. *ChemPuBSoc Europe* **20:** 5346-5357; 2014.
[21] Kimani, S.G.; Phillips, J.B.; Bruce, J.I.; MacRobert, A.J.; Golding, J.P. *Photochemistry and Photobiology* **88 (1)**: 175-187; 2012.
[22] Abdalla, M.Y. *Jordan Journal of Biological Sciences* **4:** 119-124; 2011.
[23] Griiffith, O.W. *The Journal of Biological Chemistry* **257**: 13704-13712; 1982.
[24] Drew, R.; Miners, J.O. *Biochemical Pharmacology* **33**: 2989-2994; 1984.
[25] Griiffith, O.W.; Meister, A. *The Journal of Biological Chemistry* **254**: 7558-7560; 1979.
[26] Carlioz, A.; Touati, D. *EMBO J.* **5:**623–630; 1986.
[27] Dhar, S.K.; Clair, D.K.S. *Free Radical Biology and Medicine* **52**: 2209–2222; 2012.
[28] Pelicano, H.; Martin, D.S.; Xu, R.H.; Huang, P. *Oncogene* **25:** 4633–4646; 2006.
[29] Golding, J.P.; Wardhaugh, T; Patrick, L.; Turner, M.; Phillips, J.B.; Bruce, J.I.; Kimani, S.G. *British Journal of Cancer* **109**: 976–982; 2013.
[30] Maher, J.C.; Krishan, A.; Lampidis, T.J. *Cancer Chemother Pharmacol* **53**: 116–122; 2004.
[31] Liu, H.; Savaraj, N.; Priebe, W.; Lampidis, T.J. *Biochem Pharmacol* **64:** 1745–1751; 2002.
[32] Aghaee, F.; Islamian, J.P.; Baradaran. B. *J Breast Cancer* **15(2):** 141-147; 2012.
[33] Ahmad, I.M; Abdalla, M.Y.; Aykin-Burns, N.; Simons, A.L.; Oberley, L.W.; Domann, F.E.; Spitz, D.R. *Free Radic Biol Med.* **44(5):** 826–834; 2008.
[34] Blackburn, R.; Spitz, D.; Liu, X.; Galoforo, S.; Sim, J.; Ridnour, L.A.; Chen, J.; Davis, B.; Corry, P.; Lee, Y. *Free Radical Biology & Medicine* **26:** 419 – 430, 1999.
[35] Submetted article: Tão, H.; Campos, J.R.S.; Gomes-da-Silva, L.C.; Schaberle, F.A.; Dąbrowski, J.M.; Arnaut, L.G. Pro-oxidant and antioxidant effects in Photodynamic Therapy: Cells recognize that not all ROS are alike.
[36] Townsend, D. M.; Tew, K. D.; Tapiero, H. *Biomed. Pharmacother.* **57**: 145-155; 2003.
[37] Melnikova, V. O.; Bezdetnaya, L.; Potapenko, A. Y.; Guillemin, F. *Radiat. Res.* **152**: 428-435; 1999.
[38] Bielski, B. H.; Cabelli, D. E.; Arudi, R. L.; Ross, A. B. *J. Phys. Chem. Ref. Data* **14**: 1014-1100; 1985.
[39] Liao, J. C.; Roider, J.; Jay, D. G. *Proc. Natl. Acad. Sci. USA* **91**: 2659-2663; 1994.
[40] Aft, R.L.; Zhang, F.W.; Gius, D. *Br J Cancer* **87:** 805-12; 2002.
[41] Simons, A.L.; Ahmad I.M.; Mattson, D.M.; Dornfeld, K.J.; Spitz, D.R. *Cancer Res* **67:** 3364-70; 2007.
[42] Dwarakanath, B.S.; *J Cancer Res Ther* **1:** S27-31; 2009.

Strategies to enhance Photodynamic Therapy

Joana R.S. Campos[*1], Hélder Tão[1] and Luis G. Arnaut[1]

[1] Chemistry Department, University of Coimbra, Largo Paço do Conde, 3004-531 Coimbra, Portugal

SUPPLEMENTARY INFORMATION

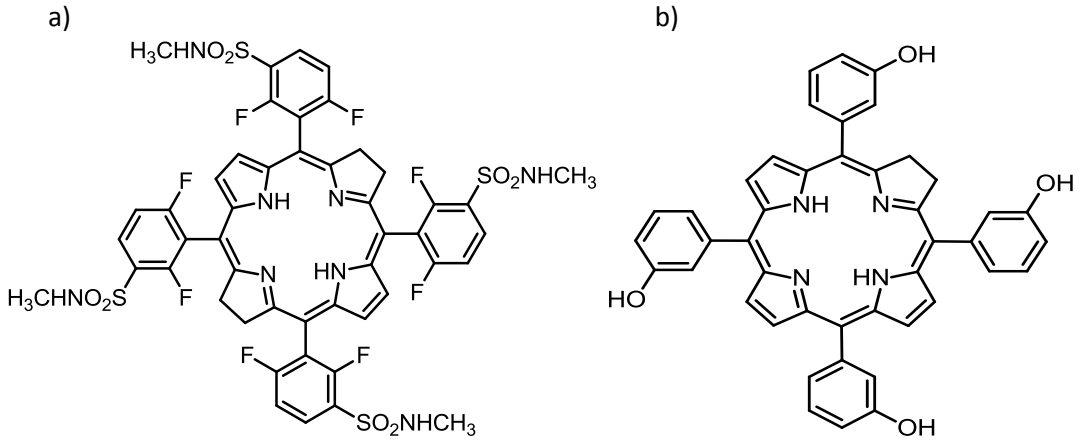

Figure 1. Molecular structure of: a)5,10,15,20-tetrakis(2,6-difluoro-3-N-methylsulfamoylphenyl) bacteriochlorin (F_2BMet or redaporfin) and b) temoporfin (*m*-tetra(hydroxyphenyl)chlorin, mTHPC).

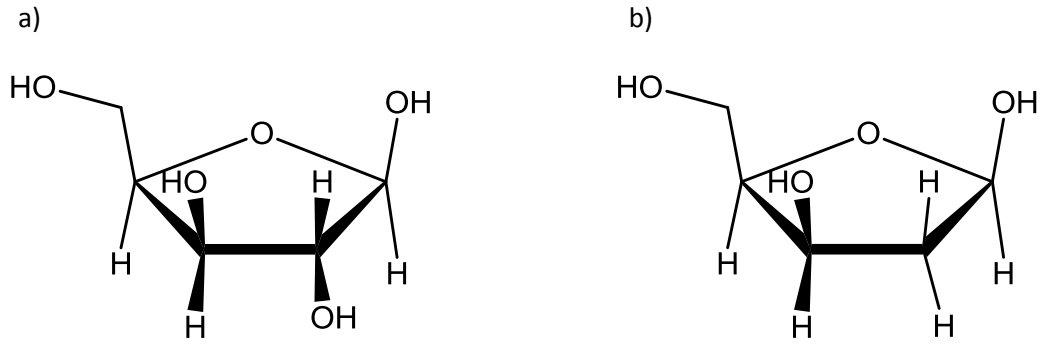

Figure 2. Molecular structure of: a) glucose and b) 2-deoxy-D-glucose (2-DG).

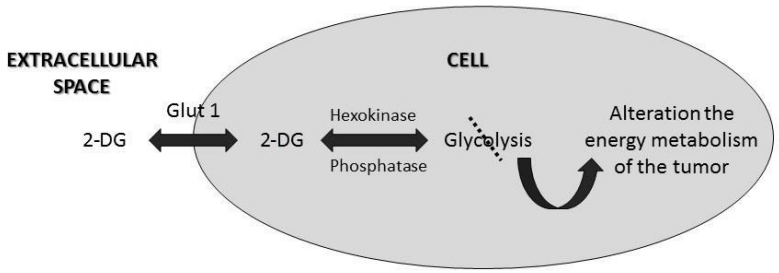

Figure 3. The inhibition of glycolysis and the preferential accumulation in cancer cells, are the basis for use 2-DG as an antitumor agent. Once inside the cell, the inhibitor will stop the glycolysis pathway and therefore alter the energy metabolism of the tumor. Adapted from *Aghaee, F.; Islamian, J. P.; Baradaran, B. Journal of Breast Cancer.* **15(2):** 141-147; 2012.

Preparation of culture medium

For 1 L of DMEM medium, 13.4 g of DMEM, 5.96 g of HEPES and 3.7 g (44.04 mmol) of sodium bicarbonate were added to 890 mL of milli-Q water, 100 mL of FBS, and 10 mL of PS. The mixture was stirred until a homogeneous solution was obtained. Solution was filtered, inside the laminar hood, through a filter with a porosity of 0.2 μm.

Measurement of the glutathione pool activity

The glutathione pool activity were measured using commercial kit from BioVision. The lysed of cells were collected and tested with commercial *Glutathione* (GSH/GSSG/Total) *Fluorometric Assay kit* from Biovision. O-Phthalaldehyde (OPA) reacts with GSH (but not with the oxidized glutathione – GSSG), generating fluorescence, and GSH can be specifically quantified. Adding a reducing agent converts GSSG to GSH, and the total GSH+GSSG pool can be determined. To measure GSSG specifically, a GSH quencher is added to remove GSH, preventing reaction with OPA (while GSSG is unaffected). The reducing agent is then added to destroy excess quencher and convert GSSG to GSH, and GSSG can be specifically quantified.

Measurement of SOD activity

For SOD, the lysed of cells were collected and tested with commercial *Superoxide Dismutase Assay kit* from Biovision. The assay utilizes WST-1 that produces a water-soluble formazan dye upon reduction with superoxide anion. The rate of the reduction with a superoxide anion is linearly related to the xanthine oxidase (XO) activity, and is inhibited by SOD. Therefore, the inhibition activity of SOD can be determined by a colorimetric method (450nm).

Measurement of absorbance

Absorbance spectra of redaporfin and temoporfin were recorded in UV-visible Recording Spectrophotometer (Shimadzu). Stock solutions of redaporfin and temoporfin were prepared in ethanol (≈ 1 mM). The samples diluted 300 times from stock solutions were measured in quartz cuvettes with an optical path of 1 cm. All measurements were performed at room temperature. Concentration of redaporfin and temoporfin solution used for all experiments was calculated using *Beer-Lambert Law*: $A = \varepsilon \, l \, c$.

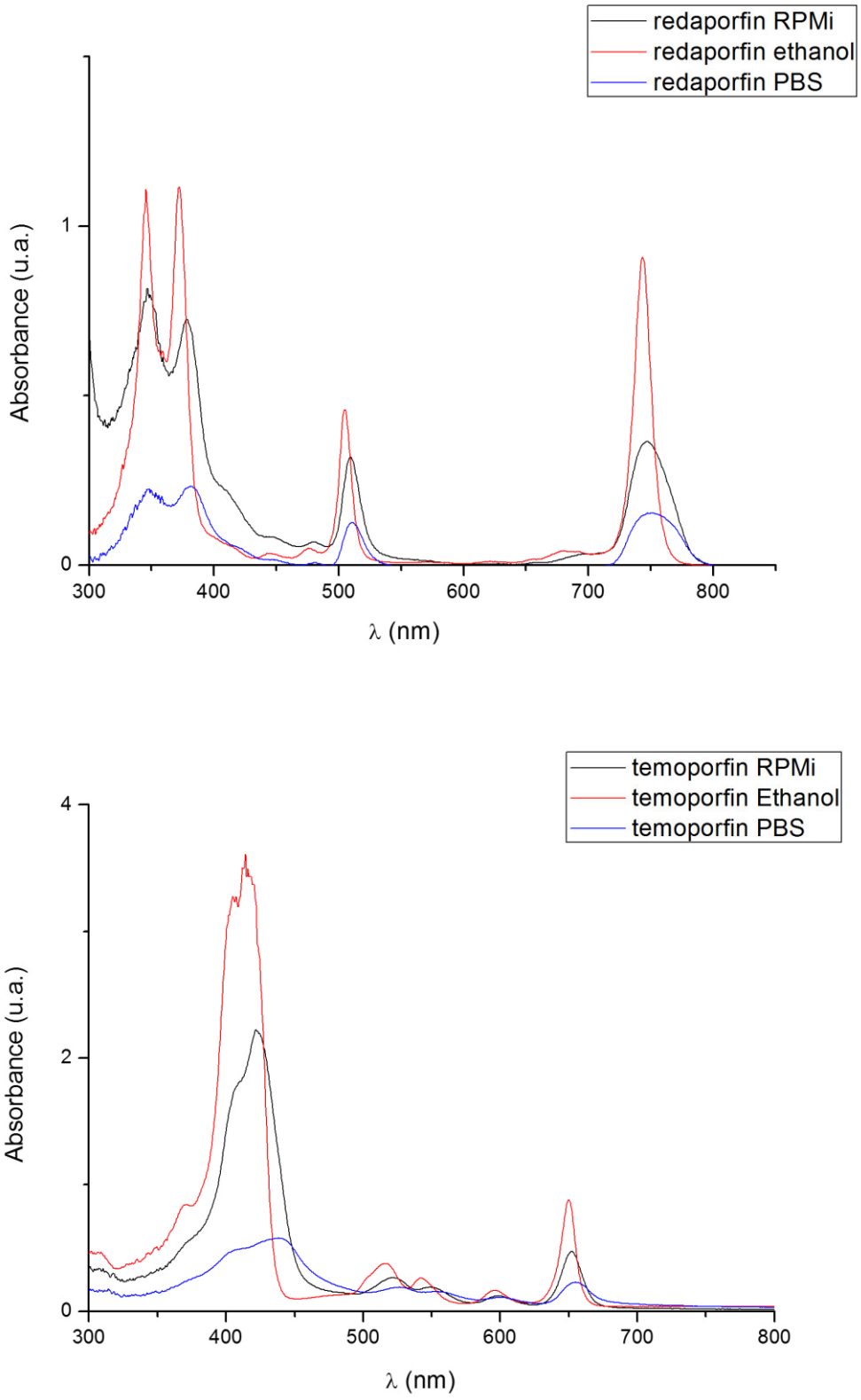

Figure 4. Absorbance normalized spectra of redaporfin and temoporfin in RPMi (black), ethanol (red) and PBS (blue).

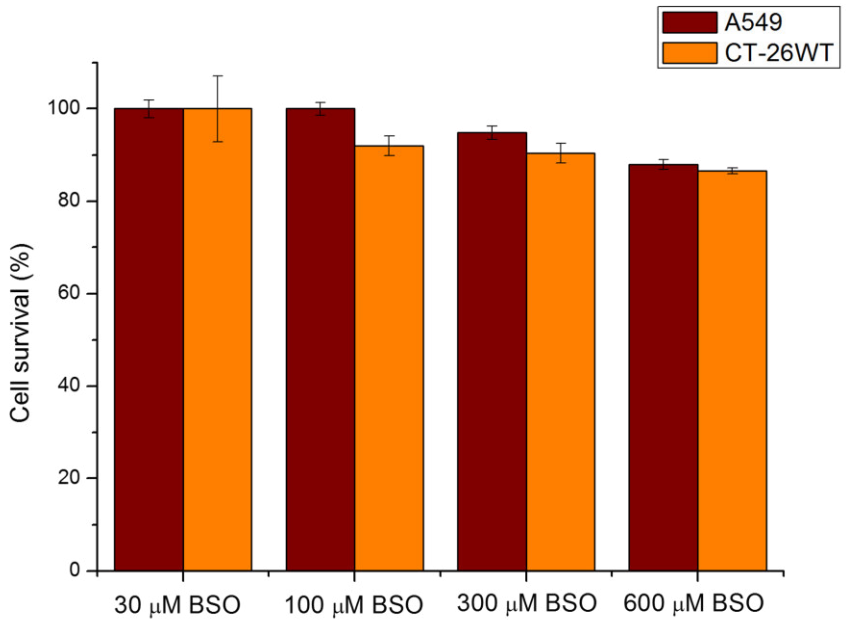

Figure 5. Cytotoxicities in the dark of BSO.

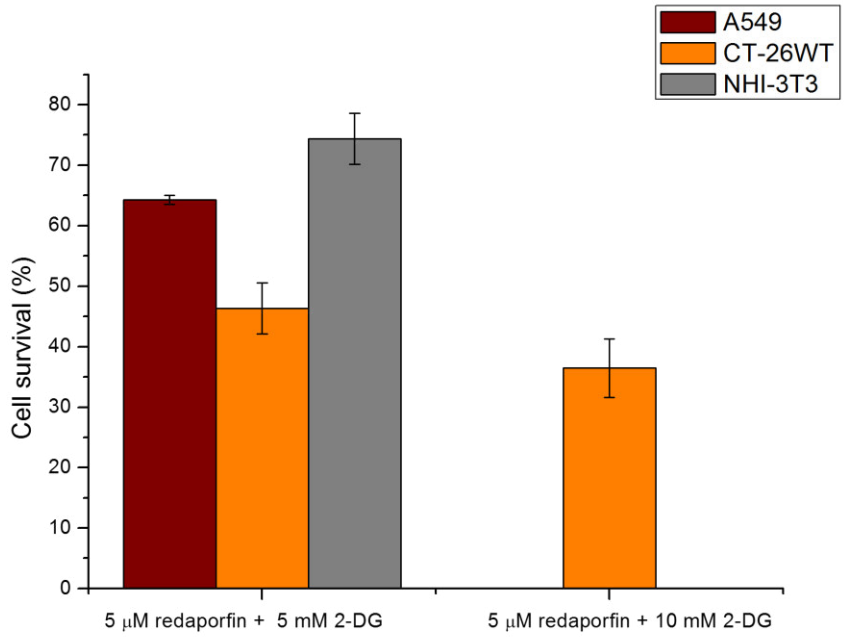

Figure 6. Dark toxicity of 5 μM redaporfin (incubated 20 h) with 5 mM and 10 mM 2-DG (incubated 48 h).

A549	Exp 1	Exp 2	Exp 3	average	stdev
redaporfin + light	41.06	46.79	43.36	43.73	2.89
redaporfin + 300 µM BSO	93.26	95.01	96.23	94.83	1.49
redaporfin + 300 µM BSO + light	42.17	46.06	43.78	44.00	1.96
redaporfin + 600 µM BSO	87.16	87.42	89.13	87.90	1.07
redaporfin + 600 µM BSO + light	30.03	34.66	32.84	32.51	2.34

Table 1. Data of dark toxicity BSO and phototoxicity of redaporfin (5 µM) alone and in combination with BSO (300 µM or 600 µM) A549 cell line.

CT26	Exp 1	Exp 2	Exp 3	average	stdev
redaporfin + light	40.57	45.20	39.72	41.83	2.95
redaporfin + 300 µM BSO	90.48	88.30	92.57	90.45	2.14
redaporfin + 300 µM BSO + light	39.75	39.067	37.16	38.66	1.34
redaporfin + 600 µM BSO	86.13	86.23	87.23	86.53	0.61
redaporfin + 600 µM BSO + light	36.53	34.23	36.23	35.66	1.25

Table 2. Data of dark toxicity BSO and phototoxicity of redaporfin (5 µM) alone and in combination with BSO (300 µM or 600 µM) CT26 cell line.

A549	GSH	average	desvpad	GT	average	desvpad	GSSG	average	desvpad
Exp 1	$1.69x10^2$	$1.89x10^2$	$2.38x10^1$	$2.36x10^3$	$2.06x10^3$	$2.70x10^2$	$1.42x10^3$	$1.34x10^3$	$0.14x10^3$
Exp 2	$1.82x10^2$			$1.98x10^3$			$1.42x10^3$		
Exp 3	$2.15x10^2$			$1.83x10^3$			$1.17x10^3$		

Table 3. Data of pool of oxidized (GSSG) and reduced (GSH) forms of glutathione and glutathione total (GT) A549 cell line.

CT26	GSH	average	desvpad	GT	average	desvpad	GSSG	average	desvpad
Exp 1	$1.69x10^2$	$1.44x10^2$	$2.15x10^1$	$1.74x10^3$	$1.79x10^3$	$6.10x10^1$	$9.43x10^2$	$9.66x10^2$	$1.15x10^2$
Exp 2	$1.35x10^2$	-	-	$1.86x10^3$	-	-	$1.09x10^3$		
Exp 3	$1.29x10^2$	-	-	$1.78x10^3$	-	-	$8.64x10^2$		

Table 4. Data of pool of oxidized (GSSG) and reduced (GSH) forms of glutathione and glutathione total (GT) CT26 cell line.

% SOD activity	Exp 1	Exp 2	average	stdev
A549	10.94	10.33	10.64	0.43
CT26	25.65	27.03	26.34	0.97

Table 5. Data of SOD activity.

Light dose mJ/cm^2	CT26 temoporfin	stdev	A549 temoporfin	stdev	CT26 redaporfin	stdev	A549 redaporfin	stdev
1	83.65	2.30	100.20	1.27	--	--	--	--
5	44.10	7.07	79.65	0.53	--	--	--	--
20	30.35	1.59	54.40	1.91	--	--	--	--
50	10.70	1.20	31.50	1.84	--	--	--	--
100	0.00	0.00	2.75	0.11	99.40	1.13	91.60	0.49
250	--	--	--	--	82.80	0.07	53.65	1.94
500	--	--	--	--	56.00	1.48	15.25	1.80
750	--	--	--	--	18.25	1.80	1.70	1.20

Table 8. Data of phototoxicity of 0.5 μM temoporfin and 5 μM redaporfin towards A549 and CT26 cells as a function of the light dose at 505 nm.

A549	Exp 1	Exp 2	Exp 3	average	stdev
redaporfin + 3 µM 2-ME	85.32	88.85	89.52	87.90	0.02
redaporfin + light	46.52	42.96	44.10	44.52	0.02
redaporfin + 3 µM 2-ME + light	20.02	20.98	19.06	20.02	0.10
redaporfin + 3 µM 2-ME + 50 µM Asc	86.32	84.40	-	85.36	0.01
redaporfin + 3 µM 2-ME + 50µM Asc + light	9.34	7.36	-	8.35	0.01
redaporfin + 50 µM asc + light	24.36	35.28	29.01	29.55	0.05

Table 6. Data of dark toxicity of 2-ME and phototoxicity of redaporfin (5 µM) alone and in combination with 2-ME (3 µM) A549 cell line.

CT26	Exp 1	Exp 2	Exp 3	average	stdev
redaporfin + 3 µM 2-ME	87.62	88.94	88.46	88.34	0.10
redaporfin + light	39.75	43.05	42.32	41.70	0.02
redaporfin + 3 µM 2-ME + light	46.44	46.44	45.22	46.04	0.10
redaporfin + 3 µM 2-ME + 50 µM Asc	86.64	85.67	-	86.15	0.10
redaporfin + 3 µM 2-ME + 50 µM Asc + light	53.17	54.10	-	53.63	0.10
redaporfin + 50 µM asc + light	56.93	55.86	56.02	56.27	0.10

Table 7. Data of dark toxicity of 2-ME and phototoxicity of redaporfin (5 µM) alone and in combination with 2-ME (3 µM) CT26 cell line.

	A549	stdev	CT26	stdev	NHI-3T3	stdev
1 mM	78.41	7.78	99.46	5.66	94.44	0.71
5 mM	82.90	6.36	98.08	4.95	68.20	0.71
10 mM	86.26	3.54	85.96	4.24	63.21	0.71
20 mM	79.46	3.54	66.56	3.06	53.95	2.12
40 mM	67.21	7.78	46.31	4.95	51.04	4.93
80 mM	58.33	2.12	45.09	10.61	45.73	2.12
100 mM	50.41	1.00	37.86	1.41	40.90	2.83

Table 9. Data of dark toxicity of 1 mM–100 mM 2-DG during 24 h.

	A549	stdev	CT26	stdev	NHI-3T3	stdev
5 µM redaporfin 5 mM 2-DG	64.29	0.71	46.33	4.24	74.36	4.24
5 µM redaporfin 10 mM 2-DG	-	-	36.46	14.85	-	-

Table 10. Data of dark toxicity of 5 µM redaporfin with 5 mM and 10 mM 2-DG during 48 h.

	A549	stdev	CT26	stdev	NHI-3T3	stdev
redaporfin + 500 µM 2DG	98.99	4.95	104.46	2.8	99.06	3.54
redaporfin + 1 mM 2DG	94.05	14.14	106.20	7.78	100.79	2.83
redaporfin + 2 mM 2DG	81.40	4.95	100.39	12.73	91.68	17.68
redaporfin	103.18	3.79	109.24	3.54	104.69	4.24
500 µM 2-DG	102.53	7.07	101.13	8.49	101.99	4.93
1 mM 2-DG	90.46	4.51	108.79	8.49	101.64	7.55
2 mM 2-DG	80.86	7.78	99.89	3.54	93.87	6.03

Table 11. Data of dark toxicity of dark toxicity of 5 µM redaporfin with 500 µM–2 mM 2-DG during 48 h.

	A549 5 mM 2-DG 80 mJ/cm²	stdev	CT26 10 mM 2-DG 130 mJ/cm²	stdev	NHI-3T3 5 mM 2-DG 25 mJ/cm²	stdev
redaporfin + light	51.28	6.36	38.51	14.14	79.52	10.60
redaporfin + 2-DG 1h + light	64.69	4.16	48.86	7.09	88.45	4.04
redaporfin + 2-DG 3h + light	72.33	5.00	68.68	2.08	90.29	1.41
redaporfin + 2-DG 6h + light	47.80	3.53	91.40	8.08	101.61	4.24
redaporfin + 2-DG 12h + light	65.70	3.53	57.25	3.21	91.72	4.72
Dark toxicity 2-DG	95.10	6.36	85.95	6.50	68.20	0.70

Table 12. Data of dark toxicity of 2-DG during 24 h and phototoxicity of redaporfin (5 µM) alone and in combination with 2-DG (5 and 10 mM) during 1, 3, 6 and 12 h before PDT.

	A549 40 mJ/cm²	stdev	CT26 100 mJ/cm²	stdev	NHI-3T3 50 mJ/cm²	stdev
redaporfin	63.29	1.69	46.11	2.76	34.82	0.42
redaporfin + 500 µM 2DG	61.75	2.61	40.82	4.57	30.71	2.02
redaporfin + 1 mM 2DG	56.31	4.81	42.04	0.71	39.86	2.04
redaporfin + 2 mM 2DG	46.89	0.01	37.06	2.59	23.99	1.34

Table 13. Data of phototoxicity of 5 µM redaporfin (incubated 20 h) alone and in combination with 500 µM–2 mM 2-DG (incubated 48 h before PDT).